Earthquake Engineering, Tenth World Conference © 1992 Balkema, Rotterdam. ISBN 90 5410 060 5

Earthquake response of retaining walls: Full scale testing and computational analysis

Ahmed-W. M. Elgamal
Department of Civil Engineering, Rensselaer Polytechnic Institute, Troy, N.Y., USA
Sreenivas Alampalli
Engineering R & D Bureau, NYS Department of Transportation, Albany, N.Y., USA

ABSTRACT: A full–scale dynamic test was conducted on a 140 ft (42.0m) long reinforced concrete cantilever retaining wall. The observed resonant configurations were similar to those of a cantilevered plate and described variability in motion along the wall height and length. A simple three dimensional (3D) finite element model was employed to further analyze these resonant configurations. It was found that such configurations may play an important role in the seismic response of wall–backfill systems of variable height (such as wing–walls). In the typical case of uniform height, seismic wall response may be evaluated by a simplified model developed for that purpose and described herein. In this model, the dynamic wall response was represented by that of a bending beam with a base rotational yielding spring and a translation slide element. A 2D shear–longitudinal beam represented the backfill soil. Using this model, a comparison was performed between the dynamic responses associated with wall base yielding in translation and in rotation.

1 INTRODUCTION

In seismically active areas, retaining structures may be subjected to substantial earthquake–induced lateral loads. In order to account for these loads, a pseudo–static procedure was introduced by Okabe (1926). Since then, numerous studies were conducted to investigate the dynamic response characteristics of wall–soil systems (Whitman, 1991). Dynamic earth pressures on small–scale laboratory models were investigated (e.g. Sherif et al., 1982). Centrifuge studies were conducted to study the seismic response of cantilever and gravity retaining walls (Ortiz et al., 1983; Steedman, 1984). Analytical and numerical models were also developed. Nazarian and Hadjian (1979) emphasize the need for a numerical model that includes a no–tension wall–soil interface, simultaneous rotation and translation of the wall base and radiation damping effects. Siddharthan et al. (1989) show that the rotational deformation (of the wall structure) may be very significant in some cases and should be accounted for in analysis procedures. Stamatopoulos and Whitman (1990) investigated the permanent tilt behavior of retaining walls. Alampalli and Elgamal (1990b; 1991) developed a simplified wall–soil computational model to investigate the permanent sliding and rotational response of cantilever and gravity retaining walls.

The results of a full–scale test conducted on a cantilever reinforced concrete wall are described herein. Impulse excitation was employed and the wall response was monitored over a wide frequency range. The measured response patterns were further analyzed with the aid of a simple 3D finite element modeling procedure. A numerical model for the seismic analysis of cantilever and gravity wall–soil systems is also presented. This model accounts for: i) wall and soil flexibility, ii) wall base sliding and rotation, iii) no–tension wall–backfill interaction, iv) nonlinear soil properties, and v) radiation damping effects. Using this model, the yielding in translation and in rotation of a cantilever wall is studied and discussed.

2 FULL–SCALE TESTING

Dynamic testing was conducted (Alampalli, 1990a) on a reinforced concrete retaining wall 140 ft. long, 1.3 ft. wide, and of a height varying between 7.5 ft. and 15.1 ft (Fig. 1). The wall supported an elevated parking lot as shown in Fig. 2.

The testing equipment (Fig. 3) consisted of a HP3562A dual channel dynamic signal analyzer, a 12 lb impulse sledge hammer (PCB model 086B50) with a force transducer, an accelerometer (PCB model 393C) to measure output acceleration, signal conditioners and a micro–computer with floppy and hard disk drives. An effort was made to keep the hammer excitation as uniform as possible for consistency. Sampling locations were chosen in such a way so as to reflect the behavior of the structure in the modes of interest (Fig. 1). Excitation input was given at each sampling point and the resulting acceleration output was measured at a stationary point on the wall (perceived not to be a modal node within the frequency range of interest). An input–output Frequency Response Function (FRF) was computed by the analyzer which also performed signal digitization using appropriate anti–aliasing filters (in real time). The process was repeated at each sampling point and the average of a number of FRFs was finally stored as the input–output transfer function for that

point. Inspection of the Coherence function (also computed by the analyzer) dictated the number of FRFs to be averaged. Almost perfectly coherent data (coherence in excess of 0.95) were recorded within the resonant frequency range of interest. A desk–top computer (HP model 300, series 9000) employed these transfer functions to compute the associated modal parameters with the aid of a modal testing package (MODAL 3.0 SE developed by Structural Measurement Systems), which assumed linearity and reciprocity for the test structure. Reciprocity was verified at selected locations by comparing frequency response functions (FRF) obtained through interchanging input and output positions. Once the modal parameters had been estimated, MODAL 3.0 SE was used to animate the calculated modal configurations of the structure for visual inspection.

Transfer functions at 178 sampling locations along the exposed side of the wall were measured. Resonant frequencies (up to 100 Hz) were obtained and sample resonant configurations of the retaining wall are shown in Fig. 4.

Fig. 4 indicates that the wall resonant configurations displayed spatial variability along the length and height. These configurations bear significant similarity to those of a cantilevered plate (3D) rather than a cantilevered beam (or 2D plane–strain analysis).

3 3D RESPONSE OF RETAINING WALLS

A finite element model was employed to further investigate the 3D dynamic response observed in full–scale (Fig. 4). The retaining wall was represented by 3D linear brick elements. A simple system of springs represented the retained soil backfill. By comparing the computed response to that recorded in full–scale, the following material properties were chosen: Young's modulus of concrete = 400,000,000 lb/ft/ft, Poisson's ratio of concrete = 0.15, and soil spring constant = 100,000 lb/ft/ft/ft. Using this modeling procedure, the response of three 150 ft long walls (Fig. 5) was studied. These walls were fixed at the base and free along the boundaries. The wall geometries (Fig. 5) were: i) a 30 ft. uniform height wall, ii) a wall of a height that varied linearly from 40 ft. to 20 ft., and iii) a wall of a height that varied linearly from 40 ft. to 10 ft. The dynamic behavior of an additional 30 ft. high plane–strain finite element model was also studied for comparison. In each case, the retained soil was assumed to extend throughout the wall height and length. The numerical models were subjected to uniform inertial excitation (to simulate the effects of uniform ground excitation) and a small amount of viscous damping was introduced to control the resulting resonant response amplitudes. A frequency sweep at an interval of 0.05 Hz was conducted with the excitation imparted in the direction perpendicular to the wall face.

The results of this sweep (Fig. 6) may be summarized as follows:

i) in the computed 2D plane–strain response, two resonant frequencies were observed. These two frequencies were associated with the first and second mode shapes of a cantilevered bending beam,

ii) the 3D 30 ft. high model also predicted two resonant frequencies, in fair agreement with its 2D counterpart, and,

iii) the two variable height walls displayed a remarkably different response pattern. In addition to the two resonant peaks that were somewhat predicted by the plane–strain model, numerous additional resonances were observed. These resonances were found to correspond to the modal configurations that describe spatial variability along the wall length (similar to the configurations of Fig. 4 that were observed in full–scale). Under the prescribed conditions of uniform inertial excitation, the 3D uniform height model displayed no such resonances. For this uniform height model, the resonant configurations with spatial variability along the wall length were perfectly symmetric, and thus resulted in a modal participation factor of zero (due to the presence of free lateral boundaries).

Consequently, it may be concluded that:

i) The seismic/dynamic response of variable height retaining walls (such as wing–walls) is more accurately modeled by a 3D formulation,

ii) For uniform height walls, the modal configurations that display spatial variability along the length will be only excited by non–uniform ground excitations. Hence, in many situations of practical significance, the seismic response of these walls may be adequately analyzed in 2D (or plane–strain).

4 MODEL FOR SEISMIC RESPONSE

Under seismic excitation, the wall was modeled to interact with the backfill soil through a system of no–tension springs (Alampalli, 1990a). Two dimensional in–plane vibration conditions were assumed (in order to represent wall–soil systems of uniform height). A bending beam represented the wall and a 2D shear–longitudinal beam represented the soil (Fig. 7). The response features of this model are discussed below, and the governing equations are presented.

4.1 Response Features of Dynamic Model

In this section, the features incorporated in this dynamic wall–soil model (see Fig. 7) are presented. Some of these features are included in currently available models and some are unique to this model. These features are:

a) Flexible wall model: A cantilevered Euler bending beam supported by a system of springs represents the wall. In many practical cases, one or two mode shapes of this beam (1 or 2 degrees of freedom) will provide sufficient accuracy in defining the dynamic wall response. These modes are easily calculated in closed form. The flexible wall model provides a realistic boundary for wall–backfill dynamic interaction. Gravity as well as cantilever walls may be modeled. In addition, a base mass may be included to simulate the wall foundation.

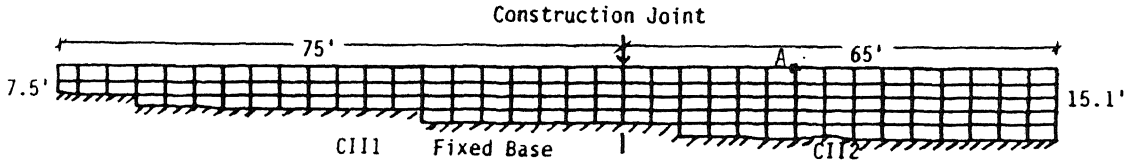

A = Location of stationary accelerometer for Impact test

Figure 1. Wall elevation with grid of response sampling locations.

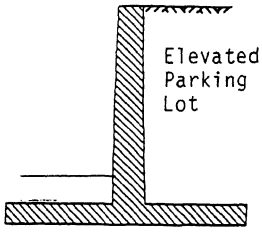

Figure 2. Schematic of wall cross-section.

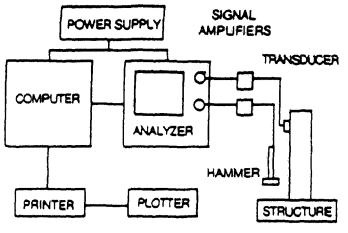

Figure 3. Schematic of test setup.

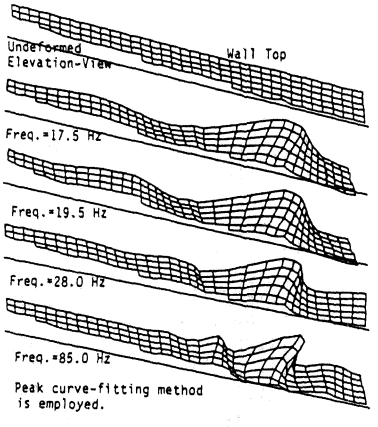

Figure 4. Sample resonant configurations of retaining wall.

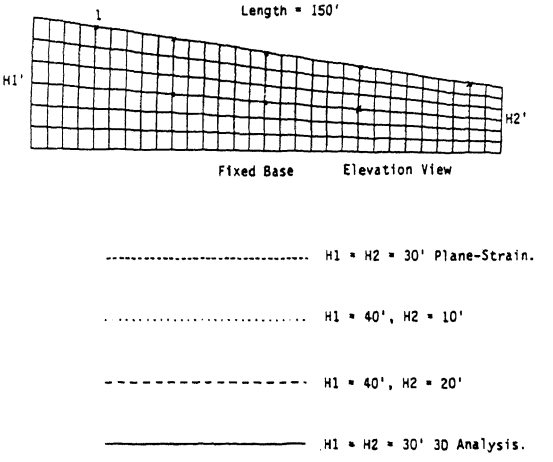

Legend used for sampled Fourier amplitude spectrum plot.

Figure 5. Schematic of wall geometries for 3D analysis.

b) Simultaneous wall translation and rotation: A translation slide element (Fig. 8) and a rotational elastic–perfectly–plastic spring (Fig. 9) are available at the retaining wall base. Thus, under dynamic loading conditions, the wall is allowed to move away from the backfill. The ultimate resistance of these yield mechanisms is equal to that available at the wall base, after subtracting the amounts necessary for static equilibrium. For example, the dynamic base yield force may be defined as:

$$F_y = \text{Static Earth Pressure Force} \times (FS - 1.0)$$

where FS = static factor of safety against sliding. It is noted that the base yield moment M_y may be either defined as described above, or else may be chosen to represent the bending resistance of a plastic hinge that could develop at the wall stem–base juncture.

c) No–tension wall–soil interface: A nonlinear spring system is chosen as a wall–soil interface (Fig. 10). No–tension properties are intended to represent the dynamic component of wall–soil interaction. These nonlinear springs are adapted to fill any gaps (partially or fully) created during transient seismic interaction. Such gaps may occur due to wall base sliding or rotation; or due to the difference in inertia and stiffness of the wall and soil systems.

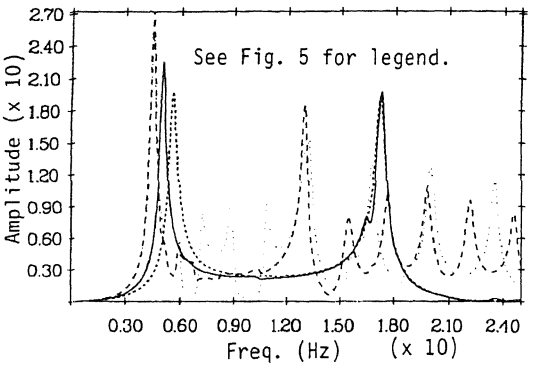

Figure 6. Fourier Amplitude spectrum at location 1 (see Fig. 5).

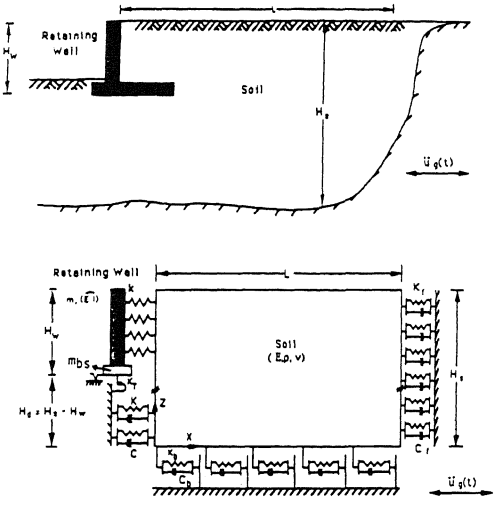

Figure 7. Wall-soil configuration and computational model.

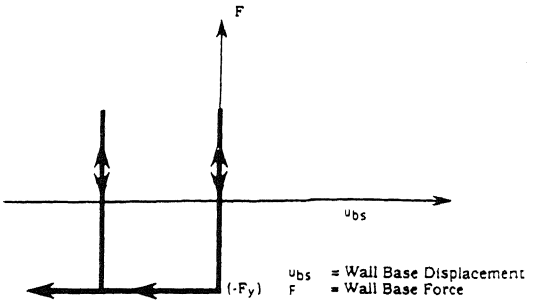

Figure 8. Wall base translational slide element.

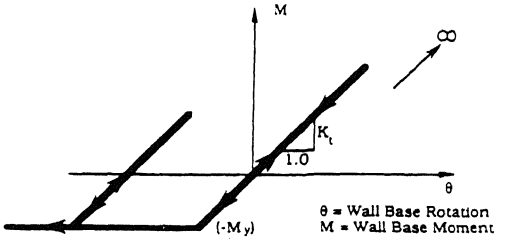

Figure 9. Wall base rotational yielding spring model.

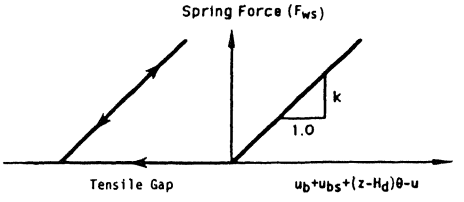

Figure 10. Wall-backfill soil interaction spring formulation.

d) Soil model with ground motion amplification: A simple soil model is proposed. Only lateral vibration is included (2D shear–longitudinal beam). As mentioned earlier, no–tension springs allow wall–backfill soil interaction. The other backfill boundaries (base and far end) are modeled by spring–dashpot mechanisms so as to account for far–field compliance and radiation damping effects. For this soil–domain model, the mode shapes are conveniently calculated in closed form. In most cases, a small number of modes (10 or less) will represent the soil response with sufficient accuracy.

e) Nonlinear soil model: The dynamic hysteretic soil response is represented by an elasto–plastic path–dependent model based on the flow or incremental theory of plasticity. An infinite yield surface formulation is implemented for that purpose.

In general, a small matrix equation (15x15 or less) will incorporate the above features and provide solutions of sufficient accuracy.

4.2 Model Formulation (Alampalli, 1990a)

The above described wall and soil models were used to represent the vibrational response of the combined wall–soil system. In the following section, a simplified version of this general wall–soil model was employed (see Fig. 11). In this simplified model, the following assumptions were made: 1) fixed soil base and far–end, and, 2) equal wall and soil–domain heights.

As mentioned earlier, the wall base will be allowed two degrees of freedom, one in translation, and one in rotation (2 equations). The remaining equations were obtained by considering the wall–soil seismically–induced interaction forces.

These equations may be expressed in the following form (following the method of weighted residuals):

$$\int_{\Omega} [\rho\, u_{,tt}\, v + G\, u_{,z}\, v_{,z} + E\, u_{,x}\, v_{,x} + \rho\, v\, u_{g'tt}]\, d\Omega$$

$$+ \int_{0}^{H} k\, [u(x=0) - u_b - u_{bs} - z\,\theta]\, v(x=0)\, dz = 0\,,$$

(Ω = Soil Spatial Domain x,z) (1)

$$\int_{0}^{H} [m\, u_{b'tt}\, v_b + E'I\, u_{b'zz}\, v_{b'zz} + m\, u_{g'tt}\, v_b$$

$$+ m\, u_{bs'tt}\, v_b + k\,\{u_b + u_{bs} + z\,\theta - u(x=0)\}\, v_b$$

$$+ m\, z\, \theta_{,tt}\, v_b]\, dz = 0 \qquad (2)$$

where, (,) denotes differentiation, x and z = spatial coordinates, ρ = soil mass density, u(x,z) = soil displacement relative to the ground, v(x,z) = weight function for soil domain, G = soil shear modulus, E = soil Young's modulus, u_g = ground displacement, t = time, H = height of soil or wall, k = wall–soil interaction spring constant, u_b = wall displacement relative to its base, u_{bs} = wall base displacement relative to the ground, θ = wall base angle of rotation (radians), v(z) = weight function for wall model, m = wall mass per unit length, and E'I = wall flexural rigidity. Finally, a matrix equation was derived by implementing a Galerkin procedure, in which u and u_b were represented in terms of the soil–domain and wall mode shapes respectively. The Newmark predictor–multi–corrector implicit scheme was employed to obtain a time domain step–by–step solution of this matrix equation. Due to the various incorporated nonlinearities, iterations were performed at each time step so as to achieve a specified convergence tolerance.

5 DYNAMIC RESPONSE OF CANTILEVER WALL–SOIL SYSTEM

In view of the virtual absence of actual recorded retaining wall strong–motion, no quantitative comparisons with actual case histories were possible. The proposed simplified numerical model was calibrated using the centrifuge test results of Bolton and Steedman (1982), who tested a fixed base micro–concrete cantilever retaining wall model at a simulated gravity field of 80g. The model represented a prototype reinforced concrete wall 14 m in height and 1.2 m in thickness. Behind the wall, a dry cohesionless backfill was placed (e=0.75, ϕ =35^{o}, and wall–soil friction angle δ = 30.0^{o}). Using the Coulomb earth pressure theory, and the measured base moment resistance, the factor of safety (FS) in overturning was estimated to be 1.26. The wall–soil model was subjected to a

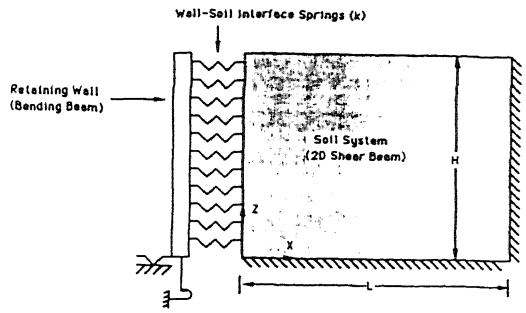

Figure 11. Simplified wall-soil model.

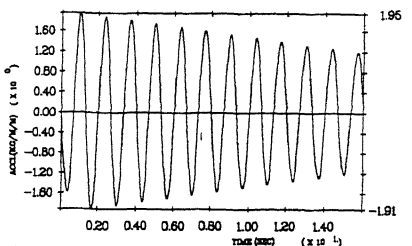

Figure 12. Input acceleration.

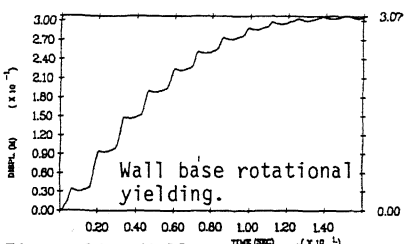

Figure 13. Wall top displacement

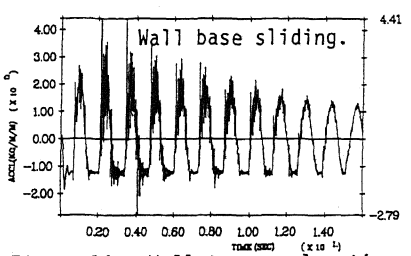

Figure 14. Wall top acceleration.

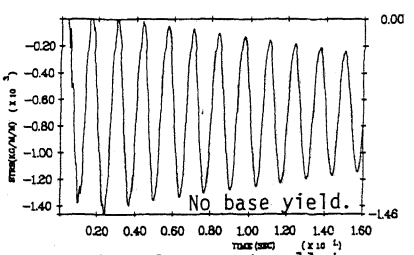

Figure 15. Stress at wall top.

predominantly harmonic input excitation (0.75 Hz) for a duration of 16 seconds (Fig. 12). Several cycles of permanent wall yield were observed due to the development of a base plastic hinge.

The numerical model was used to simulate the above mentioned centrifuge test. In this case, a rigid–plastic base rotational spring was employed (FS in overturning = 1.26). An accurate solution was computed using six beam modes and ten soil modes. The computed wall displacement history (Fig. 13) and the predicted residual value at the wall top (30 cms) were found to be in good agreement with those actually observed (28 cms).

The numerical model was then used (with the same input excitation) to study the following two additional cases:

i) Wall base translation allowed with no rotational base yielding: In this case, the same wall top displacement was obtained (30 cms) for a static FS (in translation) of 1.15 as compared with the above FS (in overturning) of 1.26. This suggests that the rotational failure mode would dominate if a wall was designed for equal factors of safety in rotation and in translation. A threshold yield acceleration of 0.12g appeared in the wall response of Fig. 14 and corresponded to the phases of wall base sliding. As in the above case of rotational yielding, a residual dynamically induced stress of about 400 kg/m/m was developed at the wall top.

ii) No wall base yielding allowed: At the end of shaking, it was found that a total wall top displacement of 1.0 cm was accumulated during the first two cycles of dynamic loading (due to wall flexibility). However, the residual dynamically induced stresses at the wall top (Fig. 15) were 1.75 times the value observed when base yielding occurred (either in rotation, or in translation). Consequently, it may be concluded that a clear reduction in the dynamically induced residual lateral stresses is associated with base yielding.

6 SUMMARY AND CONCLUSIONS

Full–scale testing was conducted on a cantilever retaining wall–soil system. The observed wall resonant configurations were similar to those of a cantilevered plate, and described variability in motion along the wall height and length. A simplified model for the seismic analysis of gravity and cantilever wall–soil systems was also presented. The model was used to investigate the yielding response of a wall–soil system, in translation, and in rotation. Computed histories of the seismically induced lateral wall acceleration, displacement and backfill–stress were shown and discussed.

7 ACKNOWLEDGEMENTS

This research was supported by the NCEER contract No. 90–1506 under NSF Master contract ECE–86–07591. The authors are indebted to Mr. Ahmed Ragheb for conducting some of the reported numerical simulations.

8 REFERENCES

Alampalli, S. 1990a. Earthquake Response of Retaining Walls: Full Scale Testing and Computational Modeling. Ph.D. Thesis, Rensselaer Polytechnic Institute, Troy, NY.

Alampalli, S., and Elgamal, A–W. 1990b. Dynamic Response of Retaining Walls Including Supported Backfill: A Computational Model. Fourth US Natl. Conf. on Earthquake Engng., Palm Springs, CA, Vol. 3, 623–632.

Alampalli, S. and Elgamal, A–W. 1991. Seismically Induced Permanent Deformations of Retaining Walls. Geotechnical Engineering Congress 1991, Geo. Special Publ. No. 27, Vol. II ASCE, Boulder, Colorado, 1174–1185.

Bolton, M.D., Steedman, R.S. 1982. Centrifugal Testing of Micro Concrete Retaining Walls Subjected to Base Shaking. Proc. Soil Dyn. and Earthq. Engng. Conf., Southampton, 311–329.

Nazarian, H.N., and Hadjian, A.H. 1979. Earthquake–Induced Lateral Soil Pressures on Structures. J. Geotech. Engng., ASCE, 105, GT9.

Okabe, S. 1926. General Theory of Earth Pressure. Journal of Japanese Society of Civil Engineers, Vol. 12, No. 1.

Ortiz, L.A., Scott, R.F., and Lee, J. 1983. Dynamic Centrifuge Testing of Cantilever Retaining Walls. J. of Earthquake Engineering and Structural Dynamics, Vol. 11, 251–268.

Sherif, M.A., Ishibashi, I., and Lee, C.D. 1982. Earth Pressures Against Rigid Retaining Walls. Journal of Geotechnical Engineering, ASCE, Vol. 108, 679–695.

Siddharthan, R., Norris, G.M., and Maragakis, E. 1989. Deformation Response of Rigid Retaining Walls to Seismic Excitation. Proc. Fourth Intl. Conf. on Soil Dynamics And Earthquake Engng., Mexico city, Mexico, 315–330.

Stamatopoulos, C.A., and Whitman, R.V. 1990. Prediction of Permanent Tilt of Gravity Retaining Wall by the Residual Strain Method. Proc. Fourth US National Conf. on Earthquake Engng, Palm Springs, CA, Vol. 3, 683–692.

Steedman, R.S. 1984. Modeling the Behavior of Retaining Walls in Earthquakes. Ph.D. Thesis, Cambridge University, Cambridge, England.

Whitman, R.V. 1991. Seismic Design of Earth Retaining Structures. Second Intl. Conf. on Recent Advances in Geotechnical Earthquake Engineering and Soil Dynamics, St. Louis, Missouri, Vol. II, 1767–1778.